frontiers in Marine Science

ORIGINAL RESEARCH
published: 12 July 2019
doi: 10.3389/fmars.2019.00364

Mesopelagic Sound Scattering Layers of the High Arctic: Seasonal Variations in Biomass, Species Assemblage, and Trophic Relationships

Maxime Geoffroy[1,2], Malin Daase[2], Marine Cusa[2†], Gérald Darnis[3], Martin Graeve[4], Néstor Santana Hernández[2], Jørgen Berge[2,5], Paul E. Renaud[5,6], Finlo Cottier[2,7] and Stig Falk-Petersen[2,6]*

[1] Centre for Fisheries Ecosystems Research, Fisheries and Marine Institute of Memorial University of Newfoundland, St. John's, NL, Canada, [2] Faculty of Biosciences, Fisheries and Economics, UiT The Arctic University of Norway, Tromsø, Norway, [3] Québec-Océan, Département de Biologie, Université Laval, Québec, QC, Canada, [4] Alfred Wegener Institute, Helmholtz Centre for Polar and Marine Research, Bremerhaven, Germany, [5] Department of Arctic Biology, The University Centre in Svalbard, Longyearbyen, Norway, [6] Akvaplan-niva, Fram Centre for Climate and the Environment, Tromsø, Norway, [7] Scottish Association for Marine Science, Oban, United Kingdom

Mesopelagic sound scattering layers (SSL) are ubiquitous in all oceans. Pelagic organisms within the SSL play important roles as prey for higher trophic levels and in climate regulation through the biological carbon pump. Yet, the biomass and species composition of SSL in the Arctic Ocean remain poorly documented, particularly in winter. A multifrequency echosounder detected a SSL north of Svalbard, from 79.8 to 81.4°N, in January 2016, August 2016, and January 2017. Midwater trawl sampling confirmed that the SSL comprised zooplankton and pelagic fish of boreal and Arctic origins. Arctic cod dominated the fish assemblage in August and juvenile beaked redfish in January. The macrozooplankton community mainly comprised the medusa *Cyanea capillata*, the amphipod *Themisto libellula*, and the euphausiids *Meganyctiphanes norvegica* in August and *Thysanoessa inermis* in January. The SSL was located in the Atlantic Water mass, between 200–700 m in August and between 50–500 m in January. In January, the SSL was shallower and weaker above the deeper basin, where less Atlantic Water penetrated. The energy content available in the form of lipids within the SSL was significantly higher in summer than winter. The biomass within the SSL was >12-fold higher in summer, and the diversity of fish was slightly higher than in winter (12 vs. 9 species). We suggest that these differences are mainly related to life history and ontogenetic changes resulting in a descent toward the seafloor, outside the mesopelagic layer, in winter. In addition, some fish species of boreal origin, such as the spotted barracudina, did not seem to survive the polar night when advected from the Atlantic into the Arctic. Others, mainly juvenile beaked redfish, were abundant in both summer and winter, implying that the species can survive the polar night and possibly extend its range into the high Arctic. Fatty-acid

OPEN ACCESS

Edited by:
Michael Arthur St. John, Technical University of Denmark, Denmark

Reviewed by:
Stein Kaartvedt, University of Oslo, Norway
Harald Gjøsæter, Norwegian Institute of Marine Research (IMR), Norway

***Correspondence:**
Maxime Geoffroy
maxime.geoffroy@mi.mun.ca

†Present Address:
Marine Cusa, School of Environment and Life Sciences, University of Salford, Greater Manchester, United Kingdom

Specialty section:
This article was submitted to Marine Ecosystem Ecology, a section of the journal Frontiers in Marine Science

Received: *12 March 2019*
Accepted: *12 June 2019*
Published: *12 July 2019*

Citation:
Geoffroy M, Daase M, Cusa M, Darnis G, Graeve M, Santana Hernández N, Berge J, Renaud PE, Cottier F and Falk-Petersen S (2019) Mesopelagic Sound Scattering Layers of the High Arctic: Seasonal Variations in Biomass, Species Assemblage, and Trophic Relationships. Front. Mar. Sci. 6:364. doi: 10.3389/fmars.2019.00364

trophic markers revealed that Arctic cod mainly fed on calanoid copepods while juvenile beaked redfish targeted krill (*Thysanoessa* spp.). The relatively high biomass of Arctic cod in August and of redfish in January thus suggests a shift within the SSL, from a *Calanus*-based food web in summer to a krill-based food web during winter.

Keywords: mesopelagic fish and zooplankton, Arctic and boreal ecosystems, seasonality, fatty acid trophic markers, *Sebastes*, Barents Sea, *Boreogadus saida*, Svalbard

INTRODUCTION

Sound scattering layers (SSL) appear on active acoustic echograms as extensive echoes above background noise resulting from aggregations of organisms in the water-column (Proud et al., 2015). Mesopelagic SSL composed of a mixture of macrozooplankton and small pelagic fish are ubiquitous in the world's oceans (Irigoien et al., 2014; Proud et al., 2018). The global biomass of mesopelagic fish is estimated to 10 billion metric tons (Irigoien et al., 2014; St. John et al., 2016) and mesopelagic organisms represent important prey for higher trophic levels (Naito et al., 2013) and a key component of the biological carbon pump through diel vertical migrations (DVM; St. John et al., 2016; Aumont et al., 2018). Scientific interest in the global distribution and, to a lesser extent, composition of the SSL has increased over the last decade, partly due to recent projects of commercially harvesting mesopelagic fish. Large-scale studies were conducted in the tropical and sub-tropical regions (Irigoien et al., 2014; Aksnes et al., 2017), Antarctica (e.g., Jarvis et al., 2010), Pacific Ocean (Benoit-Bird and Au, 2004) and the North Atlantic (Pepin, 2013; Fennell and Rose, 2015). However, knowledge on species composition and total biomass within high latitude SSL remains scarce (Siegelman-Charbit and Planque, 2016).

Recent studies documented the composition (Knutsen et al., 2017) and diel vertical migrations (Gjøsæter et al., 2017) of SSL north of Svalbard in late summer, and reported high occurrences of fish and zooplankton of boreal origin. Wassmann et al. (2015) suggested that boreal organisms advected with Atlantic Water (AW) into the Arctic cannot survive and reproduce in their new environment, which represents a literal dead-end for most advected taxa. The polar night could limit the survival of pelagic species of boreal origin in the Arctic Ocean due to inferior feeding conditions imposed by the extreme light climate (Kaartvedt, 2008). Yet, high levels of biological activity prevail during the polar night and demersal fish of Atlantic origin such as haddock (*Melanogrammus aeglefinus*) and Atlantic cod (*Gadus morhua*) feed actively in winter (Berge et al., 2015). However, it is difficult to assess if pelagic organisms survive the polar night at high latitudes as the biomass and assemblage of the SSL are, at best, poorly documented in wintertime. Such information is nonetheless critical to understand the ongoing borealization of the Arctic fish community (Fossheim et al., 2015).

The winter diet of carnivorous zooplankton and pelagic fish represents an additional knowledge gap in the high Arctic. The herbivorous calanoid copepods efficiently store large amount of lipids from their algal diet during the spring bloom of diatoms (Falk-Petersen et al., 2007) and are at the base of the pelagic food web in summer (Falk-Petersen et al., 1990). In winter, flagellates dominate the algal community (van Leeuwe et al., 2018), and most *Calanus* spp. are in diapause at depths of hundreds or thousands of meters (Dale et al., 1999; Falk-Petersen et al., 2009b). Carnivorous zooplankton and pelagic fish must then switch their diet from copepods to different prey items. Further knowledge about seasonal variations in trophic ecology is needed to increase our understanding of the energy flow through pelagic food webs in Arctic marine ecosystems (Haug et al., 2017).

We conducted acoustic-trawl surveys in the European Arctic north of Svalbard (79.8 to 81.4°N) in winters 2016 and 2017 and in summer 2016 to document seasonal and spatial variations in the distribution, species assemblage, and relative biomass of pelagic fish and macrozooplankton within the SSL. Here, we link these changes to environmental variables and assess seasonal variations in the flow of energy indicated by fatty-acid trophic markers.

MATERIALS AND METHODS

Study Area

We conducted acoustic-trawl surveys in the northern Barents Sea, north of Svalbard, on board the R/V *Helmer Hanssen* from 14 to 16 January and 28 to 29 August 2016, and from 11 to 14 January 2017. The transects aimed northwards from Rijpfjorden (22.3°E, 80.2°N), crossed the shelf and slope, and stopped at >81°N before heading south toward Smeerenburgfjorden (11.0°E, 79.8°N; **Figure 1A**). In January 2017, the ship followed the opposite direction (i.e., started close to Smeerenburgfjorden). Bottom depth ranged from <50 m close to shore to ∼2,000 m at the end of the transects.

Hydroacoustics

The keel-mounted Simrad EK60® split-beam echosounder continuously recorded hydroacoustic data at 18, 38, and 120 kHz. The ping rate was set to maximum and pulse length to 1,024 μs. The echosounder was calibrated annually (**Supplementary Table 1**) using the standard sphere method (Demer et al., 2015). A Seabird 911 Plus CTD® recorded temperature and conductivity regularly throughout the transects from which we could derive profiles of temperature and salinity, sound speed (Mackenzie, 1981), and the coefficient of absorption at each frequency (Francois and Garrison, 1982).

Acoustic data were scrutinized and cleaned with Echoview® 8. We used Echoview's algorithms to remove background noise, impulse noise, and attenuated noise signals (De Robertis and Higginbottom, 2007; Ryan et al., 2015). A minimum signal to noise ratio threshold of 10 dB was applied. Samples with a lower

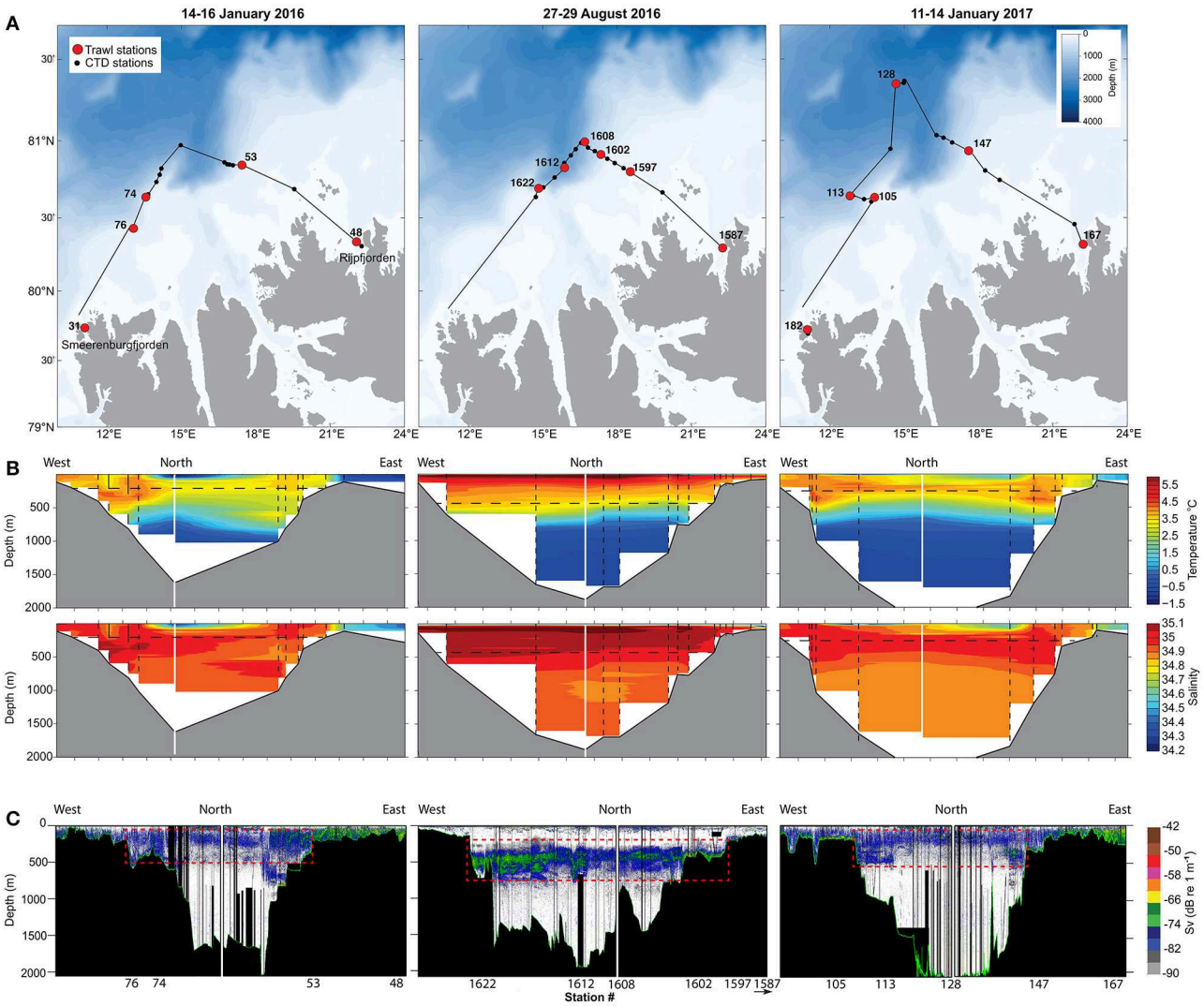

FIGURE 1 | (A) Ship's track (solid lines) and stations where the midwater trawl (red dots) and CTD (black dots) were deployed. **(B)** Temperature and salinity profiles along the ship's track. The vertical dashed lines indicate the location of the CTD profiles and the horizontal dashed lines indicate the WMD. **(C)** Echograms of volume backscattering strength (Sv) at 38 kHz. The dashed rectangles indicate SSL used in biomass calculations. Locations of the stations are indicated under the echograms.

signal to noise ratio were considered indistinguishable from background noise and were excluded from the analysis with the background noise algorithm.

Korneliussen et al. (2018) recommend to average samples before classifying targets to reduce random variability of measurements of relative frequency responses and minimize biases introduced by differences in the volume sampled at the different frequencies. The choice of analysis cell size represents a trade-off between decreasing variability in the observed relative frequency response and minimizing violations of the assumption that backscatter is dominated by a single organism (De Robertis et al., 2010). Here, the 18 and 38 kHz samples were averaged over 5 × 5 m using Echoview's "resample" algorithm. We selected the size of the cells based on previous studies on mesopelagic SSL (e.g., 5 × 5 m; D'Elia et al., 2016) and pelagic organisms in the Arctic (e.g., 5 m × 5 pings; De Robertis et al., 2010).

Due to low SNR below 200 m at 120 kHz, only the 18 and 38 kHz datasets could be used to classify acoustic targets, which reduces the classification capacity as more frequencies increase the resolution of frequency responses (Korneliussen et al., 2018). Yet, these two frequencies can provide valuable information to classify functional groups of mesopelagic scatterers. Using the difference in Mean Volume Backscattering Strength (ΔMVBS in dB re 1 m^{-1}) at 18 kHz and 38 kHz within each cell, D'Elia et al. (2016) defined a classification tree for mesopelagic organisms based on the size and categories of scatterers. We applied the same classification tree, where cells-14 dB $< \Delta MVBS_{18kHz-38kHz} < -3$ dB were assigned to crustaceans and small (1.5–15 cm) non-swimbladdered fish;

-3 dB $< \Delta MVBS_{18kHz-38kHz} < 0$ dB to large (15–60 cm) non-swimbladdered fish; 0 dB $< \Delta MVBS_{18kHz-38kHz} < 3$ dB to gelatinous zooplankton, Cephalopoda and Pteropoda; and 3 dB $< \Delta MVBS_{18kHz-38kHz} < 12$ dB to swimbladdered fish between 2.5–30 cm. Because this classification tree is based on minimum and maximum sizes and models of frequency response for each functional group rather than specific species, we could apply it to classify targets in the Arctic as long as the scattering properties and size of the organisms forming each functional group were the same. The nautical area scattering coefficient (s_A; m^2 nmi^{-2}) was then integrated over the depth of the SSL and 10-nmi wide windows for each functional group. The width of the windows was selected by plotting the standard deviation (SD) resulting from different window sizes to find the width at which the size of the windows did not impact the variance (i.e., the width at which SD reaches its asymptote). This method has the advantage of tending toward the real variance of the transects as it removes artificially high SD values resulting from a random selection of the size of the window.

For each season, the weight-based target strength function (TS_W in dB kg^{-1}; **Table 1**) of each fish and zooplankton species was calculated on the basis of its mean target strength (TS_N) and weighted mean weight in trawl samples (e.g., Benoit et al., 2008). The TS_N was calculated by feeding the weighted mean length from trawl samples into TS to length relationships (**Table 1**). We then estimated the mean integrated biomass based on the average s_A of each scattering group and on the proportion and TS_W (in the linear domain) of each species (Simmonds and MacLennan, 2005). To focus on mesopelagic SSL and avoid biases from shallower coastal areas, we discarded coastal areas <200 m and only used stations and acoustic data outside of Smeerenburgfjorden and Rijpfjorden for biomass calculations. We calculated the Weighted Mean Depth (WMD) of the SSL for each survey to document seasonal changes in vertical distribution (e.g., Knutsen et al., 2017).

Fish and Zooplankton Sampling

We deployed a Harstad pelagic trawl within the SSL to groundtruth the acoustic signal. Five to six pelagic trawl deployments were conducted for a period varying from 20–80 min at ca. three knots during each survey (**Figure 1A** and **Supplementary Table 2**). The Harstad trawl had an opening of 18.28 × 18.28 m and an effective height of 9–11 m and width of 10–12 m at 3 knots. The mesh size of the inner liner of the cod end was 10 mm. All organisms were identified to species or genus onboard. We recorded the total number and weight of each species. When >30 specimens of a given species were collected, we measured and weighted a subsample of 30 individuals. To identify spatial and seasonal changes in the SSL community, a cluster analysis using the unweighted pair-group average method with arithmetic means and the Bray–Curtis similarity index was conducted following the multivariate approach described by Darnis et al. (2008). Biomass of each taxon was expressed as a proportion of total catch at each station. Data were transformed (arcsin square-root) prior to the production of the similarity matrix to reduce the weight of highly abundant species and increase the impact of species likely to have been under-sampled (e.g., decapod species, gelatinous zooplankton such as cnidarians, and ctenophores). Verification of station groupings was strengthened using a non-metric multidimensional scaling analysis (NMDS) applied to the same similarity matrix. A similarity of percentages (SIMPER) analysis conducted with the software PRIMER V.6 identified the taxa most responsible for the intragroup similarity and dissimilarity among pelagic assemblages. We used all stations for the multivariate analysis.

This study was conducted with permission from the Governor in Svalbard and followed the strict regulations regarding health, environment and safety enforced at UNIS and UiT The Arctic University of Norway. This study was carried out in accordance with the Norwegian animal welfare act and was approved by the Department of Arctic and Marine Biology at UiT.

Lipid Analysis

We analyzed the concentrations of Fatty Acid Trophic Markers (FATM) to document seasonal variations in energy flow between pelagic trophic levels (Dalsgaard et al., 2003). Subsamples of the most abundant vertebrate and invertebrate species (i.e., *Sebastes mentella*, *Boreogadus saida*, *Leptoclinus maculatus*, *Benthosema glaciale*, *Arctozenus risso*, *Clupea harengus*, *Themisto libellula*, *Thysanoessa inermis*, and *Meganyctiphanes norvegica*) were frozen at −80°C for lipid analysis. We analyzed five to ten individuals of each of these species for 37 fatty acid (FA) and 8 fatty alcohol (Falc) compositions via gas chromatography (Kattner and Fricke, 1986). The sum of FA and Falc was expressed as total lipids. The concept of FATM is based on the knowledge that FA and Falc patterns characterize specific taxa of primary producers and zooplankton species, and that the patterns are transferred relatively unchanged through the food chain. Based on the FA and Falc composition, several biomarker ratios have been calculated. Here, the 18:1(n-9)/18:1(n-7) ratio indicated carnivory in zooplankton (Graeve et al., 1997; Auel et al., 2002), while 20:5(n-3)/22:6(n-3) and 16:1(n-7)/16:0 ratios differentiated diatom and flagellate based diets, respectively (Graeve et al., 1994). We used the highly polyunsaturated vs. saturated fatty acids ratio (PUFA/SAFA) to track the flow of energy, and the 22:1(n-11)/20:1(n-9) ratio to differentiate within diets based on *Calanus* species (∼1.8 or higher refers to *C. hyperboreus*, 1.1 to *C. finmarchicus*, and 0.7 or lower to *C. glacialis*) (Falk-Petersen et al., 1990, 2007).

To assess differences in FATM composition among different species, we conducted a multivariate analysis of fatty acids using a correspondence analysis (CA) (Greenacre, 2016). Correspondence analyses are suitable for compositional data in the presence of a large number of zeros (Greenacre, 2016). A centroid discriminant analysis was conducted to discriminate between the species energy content and dietary derived fatty acids (i.e., structural fatty acids vs. copepod-derived long-chain fatty acids). Computations were conducted with the R package *ca* (Nenadić and Greenacre, 2007).

TABLE 1 | Details of all mesopelagic organisms sampled offshore (bottom depth >200 m).

Species	Origin	Total biomass in trawls (g)	Total number of individuals in trawls	Weighted mean length (cm) ± ME	TS_W (dB kg^{-1})	Mean acoustic biomass (g nmi^{-2})	SD (g nmi^{-2})	Reference for TS calculations
January 2016								
Sebastes sp.	Boreal	2,672.0	1270	6.52 ± 0.12	−23.45	537,217.9	191,873.0	(Gauthier and Rose, 2002)
Cyanea capillata	Cosmopolitan	5,683.0	40	-	−58.03	503,235.0	132,755.2	Central value from the TS range in (Crawford, 2016)
Mallotus villosus	Boreal	186.0	23	12.98 ± 1.57	−16.83	37,396.2	13,356.4	(Rose, 1998)
Thysanoessa spp. (mainly *T. inermis*)	Boreal and Arctic	840.9	3910	2.16 ± 0.21	−58.41	28,489.3	14,909.1	Fluid-like equation from (Stanton et al., 1994)
Melanogrammus aeglefinus	Boreal	68.0	2	16.75	−58.20	13,671.7	4,883.0	(Foote, 1987)
Boreogadus saida	Arctic	54.6	23	7.65 ± 0.61	−26.15	10,967.5	3,917.2	(Geoffroy et al., 2016)
Meganyctiphanes norvegica	Boreal	139.6	609	1.33 ± 0.50	−69.43	4,729.6	2,475.1	Fluid-like equation from (Stanton et al., 1994)
Myctophidae *(Notoscopelus kroyeri* and/or *Benthosema glaciale)*	Boreal and Arctic	16.8	16	4.64 ± 0.51	−64.10	3,377.7	1,206.4	(Scoulding et al., 2015)
Cnetophores	Cosmopolitan	33.0	14	2.05 ± 1.18	−57.02	2,922.2	770.9	Fluid-like equation from (Stanton et al., 1994)
Themisto libellula	Arctic	84.6	245	2.08 ± 0.78	−47.99	2,866.2	1,500.0	Fluid-like equation from (Stanton et al., 1994)
Gonatus fabricii	Boreal	29.8	4	9.27	−57.66	2,634.4	695.0	Fluid-like equation from (Stanton et al., 1994)
Gadus morhua	Boreal	8.3	1	11.40	−24.05	1,668.8	596.0	(Rose and Porter, 1996)
Pandalus borealis	Boreal and Arctic	43.8	10	5.31 ± 3.80	−56.15	1,483.9	776.6	Fluid-like equation from (Stanton et al., 1994)
Leptoclinus maculatus	Boreal and Arctic	26.7	31	7.44 ± 0.37	−39.35	904.6	473.4	Equation for elongated non-swimbladdered fish in (Gauthier and Horne, 2004)
Themisto abyssorum	Boreal and Arctic	12.3	184	0.98 ± 0.35	−50.75	415.0	217.2	Fluid-like equation from (Stanton et al., 1994)
Pasiphaea sp.	-	2.8	2	5.31	−51.20	94.9	49.6	Fluid-like equation from (Stanton et al., 1994)
Unidentified isopod	-	0.3	1	-	-	-	-	
Lebbeus polaris	Boreal and Arctic	0.2	1	-	-	-	-	
Unidentified siphonophore	-	0.2	1	-	-	-	-	
Total		9,902.8	6,387	-	-	**1,152,074.8**	**370,454.0**	
August 2016								
Themisto libellula	Arctic	7,440.0	68,843	1.62 ± 0.60	−48.46	18,935,929.7	10,520,636.1	Fluid-like equation from (Stanton et al., 1994)
Meganyctiphanes norvegica	Boreal	2,088.6	16,256	2.25 ± 0.84	−54.67	5,315,676.9	2,953,343.3	Fluid-like equation from (Stanton et al., 1994)

(Continued)

TABLE 1 | Continued

Species	Origin	Total biomass in trawls (g)	Total number of individuals in trawls	Weighted mean length (cm) ± ME	TS_W (dB kg^{-1})	Mean acoustic biomass (g nmi^{-2})	SD (g nmi^{-2})	Reference for TS calculations
Cyanea capillata	Cosmopolitan	805.8	17	-	−53.26	1,750,802.2	1,585,955.0	Central value from the TS range in (Crawford, 2016)
Boreogadus saida	Arctic	479.4	102	8.78 ± 1.12	−27.55	1,481,716.7	1,376,606.8	(Geoffroy et al., 2016)
Thysanoessa spp. (mainly *T. inermis*)	Boreal and Arctic	329.4	3,089	2.95 ± 0.13	−65.83	838,245.8	465,722.0	Fluid-like equation from (Stanton et al., 1994)
Gonatus fabricii	Boreal	244.2	25	9.27 ± 3.49	−58.85	530,629.1	480,667.6	Fluid-like equation from (Stanton et al., 1994)
Arctozenus risso	Boreal	363.7	13	23.18 ± 2.75	−40.89	461,276.5	325,834.1	Equation for elongated non-swimbladdered fish in (Gauthier and Horne, 2004)
Myctophidae (Notoscopelus kroyeri and/or *Benthosema glaciale)*	Boreal and Arctic	122.9	161	3.97 ± 0.19	−35.30	379,741.1	352,803.1	(Scoulding et al., 2015)
Sebastes sp.	Boreal	110.0	131	3.76 ± 0.10	−23.05	340,020.5	315,900.2	(Gauthier and Rose, 2002)
Melanogrammus aeglefinus	Boreal	105.9	16	6.81 ± 0.27	−26.64	327,192.5	303,982.1	(Foote, 1987)
Leptoclinus maculatus	Boreal and Arctic	38.6	1,096	5.95 ± 0.15	−40.65	98,115.6	54,512.2	Equation for elongated non-swimbladdered fish in (Gauthier and Horne, 2004)
Reinhardtius hippoglossoides	Boreal and Arctic	36.9	23	5.56 ± 0.31	−38.72	93,788.8	52,108.3	Equation for thick non-swimbladdered fish in (Gauthier and Horne, 2004)
Gadus morhua	Boreal	29.3	19	5.36 ± 0.79	−23.20	90,569.1	84,144.3	(Rose and Porter, 1996)
Anarhichas lupus	Boreal	18.1	5	6.29 ± 0.76	−47.20	45,940.0	25,523.9	Equation for elongated non-swimbladdered fish in (Gauthier and Horne, 2004)
Themisto abyssorum	Boreal and Arctic	16.9	289	0.58 ± 0.22	−62.14	42,885.8	23,827.0	Fluid-like equation from (Stanton et al., 1994)
Pasiphaea spp.	-	4.2	7	3.85 ± 3.56	−54.42	10,740.5	5,967.4	Fluid-like equation from (Stanton et al., 1994)
Icelus bicornis	Arctic	2.7	2	4.08	−40.20	6,871.9	3,818.0	Equation for wide non-swimbladdered fish in (Gauthier and Horne, 2004)
Aglantha digitale	Boreal and Arctic	2.2	10	1.22 ± 0.87	−56.01	4,780.1	4,330.0	Fluid-like equation from (Stanton et al., 1994)
Pandalus borealis	Boreal and Arctic	0.9	1	3.85	−56.16	2,290.6	1,272.7	Fluid-like equation from (Stanton et al., 1994)
Clione limacina	Boreal and Arctic	0.5	2	0.68	−64.84	1,086.4	984.1	Gastropod equation from (Stanton et al., 1994)
Leptagonus decagonus	Boreal and Arctic	0.4	1	3.90	−43.88	890.8	494.9	Equation for elongated non-swimbladdered fish in (Gauthier and Horne, 2004)

(Continued)

TABLE 1 | Continued

Species	Origin	Total biomass in trawls (g)	Total number of individuals in trawls	Weighted mean length (cm) ± ME	TS_W (dB kg^{-1})	Mean acoustic biomass (g nmi^{-2})	SD (g nmi^{-2})	Reference for TS calculations
Total		12,240.1	90,108	-	-	**30,759,190.7**	**18,938,432.9**	
January 2017								
Euphausiacea (mainly *T. inermis*)	Boreal and Arctic	956.0	8,392	2.74 ± 1.02	−49.81	706,268.9	532,572.7	Fluid-like equation from (Stanton et al., 1994)
Sebastes sp.	Boreal	343.3	131	5.82 ± 0.09	−25.37	641,528.3	224,496.2	(Gauthier and Rose, 2002)
Cyanea capillata	Cosmopolitan	267.3	40	-	−44.75	357,621.6	185,433.4	Central value from the TS range in (Crawford, 2016)
Gonatus fabricii	Boreal	210.1	11	9.27 ± 6.23	−62.01	281,093.5	145,752.2	Fluid-like equation from (Stanton et al., 1994)
Themisto libellula	Arctic	323.7	1,752	2.11 ± 0.79	−45.24	239,141.5	61,000.5	Fluid-like equation from (Stanton et al., 1994)
Pandalus borealis	Boreal and Arctic	114.4	83	5.31 ± 1.98	−51.13	84,515.9	21,558.4	Fluid-like equation from (Stanton et al., 1994)
Myctophidae *(Notoscopelus kroyeri* and/or *Benthosema glaciale)*	Boreal and Arctic	27.0	29	4.24 ± 0.23	−36.21	50,361.7	17,623.6	(Scoulding et al., 2015)
Leptoclinus maculatus	Boreal and Arctic	63.3	81	6.98 ± 0.16	−40.54	46,764.5	11,928.7	Equation for elongated non-swimbladdered fish in (Gauthier and Horne, 2004)
Mallotus villosus	Boreal	13.8	2	10.45	−31.71	25,788.2	9,024.3	(Rose, 1998)
Boreogadus saida	Arctic	5.2	2	7.00	−27.17	9,717.3	3,400.5	(Geoffroy et al., 2016)
Themisto abyssorum	Boreal and Arctic	6.9	89	1.14 ± 0.43	−50.76	5,097.5	1,300.3	Fluid-like equation from (Stanton et al., 1994)
Gammarus wilkitzkii	Arctic	6.8	16	2.89 ± 1.54	−36.28	5,023.7	1,281.4	Fluid-like equation from (Stanton et al., 1994)
Mertensia ovum	Boreal and Arctic	3.3	3	2.03	−52.94	4,348.2	2,254.6	Fluid-like equation from (Stanton et al., 1994).
Beroe cucumis	Boreal and Arctic	3.3	3	3.74	−45.04	4,348.2	2254.6	Fluid-like equation from (Stanton et al., 1994).
Clione limacina	Boreal and Arctic	2.9	26	1.74 ± 0.70	−49.88	3,813.0	1,977.1	Gastropod equation from (Stanton et al., 1994)
Liparis fabricii	Boreal and Arctic	1.7	1	5.90	−42.51	3,176.8	1,111.7	Equation for wide non-swimbladdered fish in (Gauthier and Horne, 2004)
Acanthostepheia malmgreni	Boreal and Arctic	2.4	13	2.08 ± 0.89	−45.27	1,773.1	452.3	Fluid-like equation from (Stanton et al., 1994)
Sergestes arcticus	Atlantic and Arctic	1.6	3	4.30	−51.33	1,145.1	292.1	Fluid-like equation from (Stanton et al., 1994)
Total		2,353.050	1,067	-		**2,471,526.9**	**1,223,714.7**	

Total biomass and number of individuals in midwater trawls are summed for each season and species. The mean acoustic biomass is calculated from the mean s_A, the weight-based target strength (TS_W), and the proportion of each species for each season. References for the Target Strength (TS) to length relationships and the origins of all species are indicated. Total mean acoustic biomass and SD for each season are written in bold.

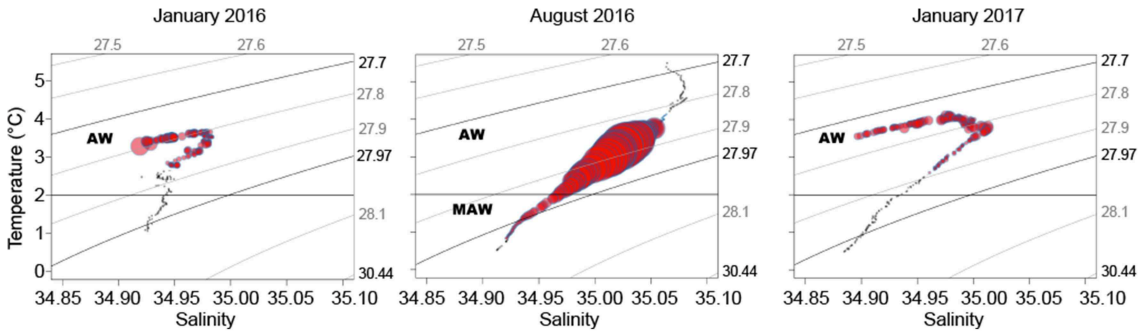

FIGURE 2 | Temperature-salinity diagrams averaged for each season with a 5-m vertical resolution. Bubble size indicates the distribution of the pelagic organisms in the SSL and is proportional to the nautical area scattering coefficient at 38 kHz (s_A; m^2 nmi^{-2}) averaged over the same 5-m strata. Isopycnals indicate potential density (kg m^{-3}) and the regions corresponding to Atlantic Water (AW) and Modified Atlantic Water (MAW) are indicated (based on water mass characteristics in Meyer et al., 2017).

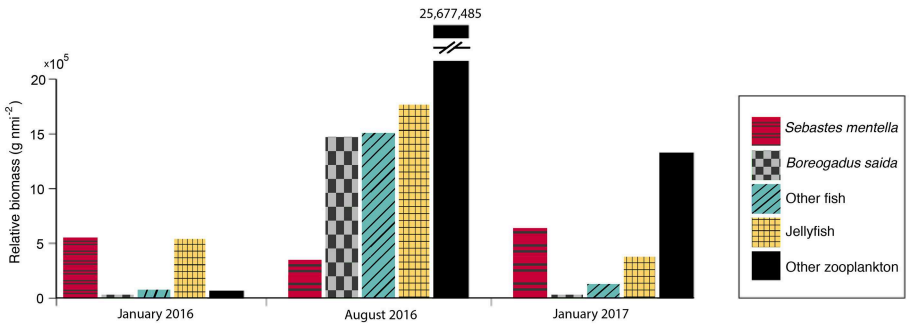

FIGURE 3 | Bar charts of the mean integrated biomass within the SSL for each season.

RESULTS

Water Masses and Vertical Distribution of the SSL

All sampling was conducted in ice-free waters, except in August 2016 when the ice edge was located around 81.0°N and the northernmost part of the transects reached very open to open drift ice. In January, the Atlantic Water mass [AW; 27.70 < σ_o <27.97 and θ > 2°C; (Meyer et al., 2017)] occupied the surface to ∼700 m above the slope and between ∼100 and ∼500 m offshore, where bottom depth was >1000 m (**Figure 1B**). Polar surface water and warm polar surface water (σ_o <27.70) occupied the top 100 m in offshore regions. In August, the AW was located between ∼50 and ∼570 m and warm polar surface water (σ_o <27.70 and θ > 2°C; Meyer et al., 2017) occupied the top 50 m (**Figure 1B**). Modified Atlantic Water (MAW; 27.70 < σ_o <27.97 and θ < 2°C; Meyer et al., 2017) was located below the AW in January and August (**Figure 1B**).

The WMD of the SSL was 221 m in January 2016, 455 m in August 2016, and 251 m in January 2017, indicating that the vertical distribution of the SSL was >200 m deeper in summer than in winter. In January, the SSL was located in the AW, from ∼50 to ∼500 m above the slope and between ∼50 and ∼250 m above the deeper basin (**Figure 1C**), which corresponded to temperatures between 2.8 and 4°C (**Figure 2**). Hence, the WMD of the SSL in January was mainly driven by organisms above the slope and the animals present above the deep basin were rather epipelagic (**Figure 1C**). The average s_A at 38 kHz within the SSL was 57 m^2 nmi^{-2} in January 2016 and 56 m^2 nmi^{-2} in January 2017. As for the WMD, the backscatter diminished above the deeper basin where less AW penetrated (≤42 m^2 nmi^{-2} in 2016 and ≤51 m^2 nmi^{-2} in 2017 for the region north of 81.9°N). Pelagic organisms generally avoided the colder polar waters and MAW in January. In August, the average s_A within the SSL was 351 m^2 nmi^{-2}. The SSL was concentrated in the lower part of the AW and in the MAW, between 200 m and 700 m (**Figure 1C**) at temperatures between 1 and 4°C (**Figure 2**).

Composition of the SSL

We sampled a total of nine fish species in the mesopelagic SSL (offshore regions) in January. Juvenile redfish (mainly the beaked redfish *Sebastes mentella*) dominated the pelagic fish assemblage (**Figure 3**). They represented 89% of the fish biomass with a mean standard length (SL) of 6.5 cm in 2016, and 83% of the biomass with a mean SL of 5.8 cm in 2017 (**Table 1**). Arctic cod (*Boreogadus saida*), referred to as polar cod in Europe, represented < 2% of the biomass in January, and had an average length of 7.6 cm (2016) and 7.0 cm (2017). The

rest of the winter fish assemblage was composed of capelin (*Mallotus villosus*), juvenile haddock, Myctophidae (*Benthosema glaciale* and *Notoscopelus kroyeri*), juvenile Atlantic cod, and juvenile daubed shanny (*Leptoclinus maculatus*) in 2016, and of Myctophidae, juvenile daubed shanny, capelin, and juvenile gelatinous snailfish (*Liparis fabricii*) in 2017 (**Table 1**). Herring (*Clupea harengus*) were sampled in Smeerenburgfjorden and Rijpfjorden. Gelatinous zooplankton, mainly *Cyanea capillata,* dominated the zooplankton assemblage in January 2016 (93% of the biomass; **Figure 3**) and represented 22% in January 2017. Euphausiids (mainly *Thysanoessa inermis*), the cephalopod *Gonatus fabricii*, and the amphipod *Themisto libellula* comprised most of the remaining macrozooplankton (**Table 1**).

Twelve fish species were sampled in the SSL in August: Arctic cod, spotted barracudina (*Arctozenus risso*), Myctophidae (*Benthosema glaciale* and *Notoscopelus kroyeri*), juvenile redfish, juvenile haddock, juvenile daubed shanny, juvenile Greenland halibut (*Reinhardtius hippoglossoides*), juvenile Atlantic cod, juvenile Atlantic wolfish (*Anarhichas lupus*), two-horn sculpin (*Icelus bicornus*), and Atlantic poacher (*Leptagonus decagonus*). Juvenile redfish represented 10% of the fish biomass and had an average length of 3.8 cm, while Arctic cod represented 45% of the biomass with an average length of 8.8 cm (**Table 1**). *Themisto libellula* and *Meganyctiphanes norvegica* strongly dominated the pelagic assemblage in August. The total fish and macrozooplankton biomass was >12 fold higher in August than January (30,759 kg nmi^{-2} vs. 1,152 kg nmi^{-2} in January 2016 and 2,472 kg nmi^{-2} in January 2017, **Table 1** and **Figure 3**).

The cluster analysis indicates three distinct station groups (**Figure 4A**). Group 1 is composed of the two Smeerenburgfjorden stations sampled in January 2016 and 2017. Group 2 comprises the other stations (7) sampled in

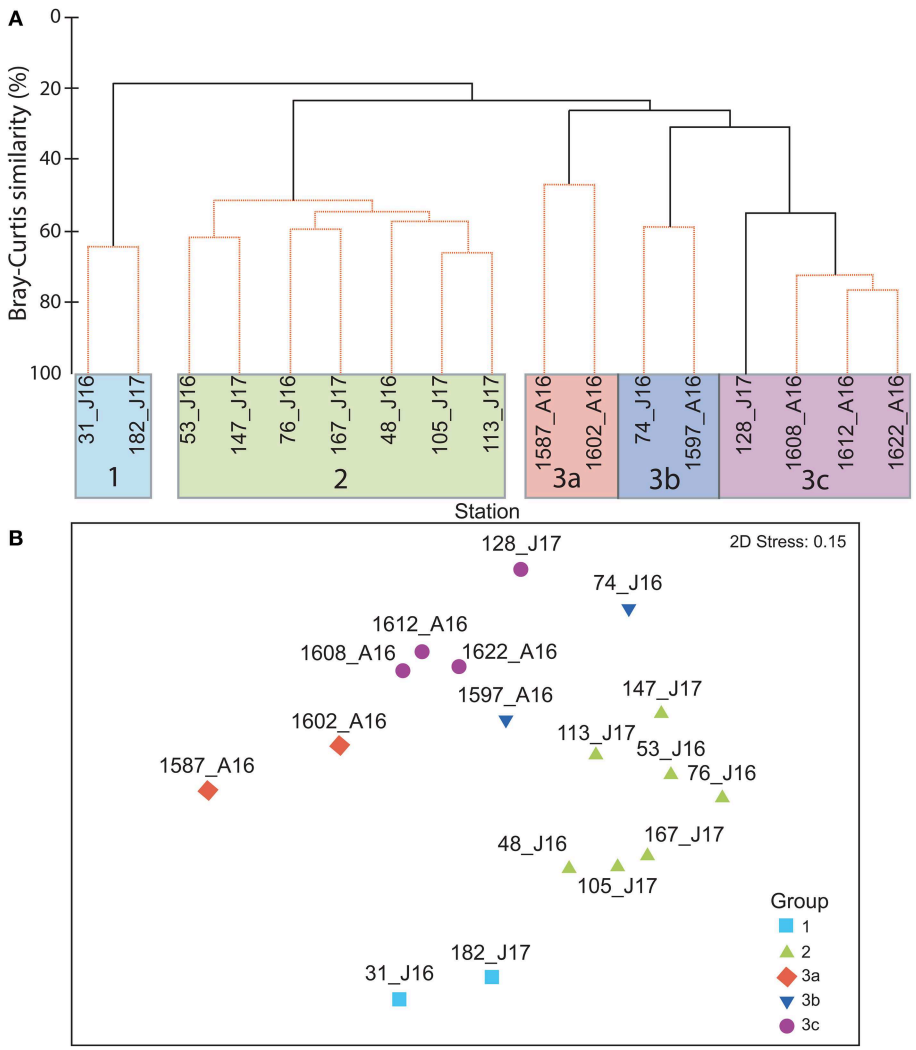

FIGURE 4 | (A) Grouping of stations based on the relative biomass of fish and zooplankton taxa in midwater trawls. **(B)** Non-metric multidimensional scaling ordination plot illustrating similarities among stations in terms of catch composition. The 3 main groups of stations identified by the cluster analysis are shown. Each station is identified by its number, the month (A = August and J = January), and year (16 = 2016 and 17 = 2017).

January 2016 and 2017, except for two stations located above the slope. The latter are included in group 3 which also includes all the stations (6) sampled in August. Group 3 presents an average low intragroup similarity compared to the other groups (38%, 54 and 64% in groups 3, 2, and 1, respectively; SIMPER) and divides into the sub-groups 3a,b,c. Groups 3a and b constitute two pairs of stations shallower than 500 m, whereas group 3c includes the northernmost stations at >1,500 m bottom depth. The NMDS analysis illustrates well the partitioning of groups, and also the wide extension of the stations making group 3 in a 2-dimensional ordination, which is indicative of comparatively low faunal similarity of its stations (**Figure 4B**). The dominance of the biomass by redfish and *Thysanoessa* spp. in winter and by *T. libellula* and *M. norvegica* in summer explains to a large extent the dissimilarity among the stations from January (group 2) and August (group 3a,b,c) (**Supplementary Table 3**). The main causes for differentiation of group 1 (Smeerenburgfjorden) are the high biomass of Arctic cod, capelin and *Pandalus borealis* present in that fjord. *Cyanea capillata* contributes heavily to the intragroup similarity of sub-groups 3a and b, whereas *T. libellula* and *M. norvegica* characterize sub-group 3c. There is no clear coastal-offshore gradient, except for the higher abundance of Arctic cod and northern shrimp in Smeerenburgfjorden, and the sub-group 3c made of stations deeper than 1,500 m.

Lipid Composition

The nine species analyzed for lipids contained thirty FA and four Falc (**Table 2**). The first (horizontal) axis of the correspondence/discriminant analysis (CA/DA) ordination plot (**Figure 5**) explains 80.4% of the variation in the FA composition and four groups were identified. Organisms forming groups 1-3 dominated the biomass in summer and, except for spotted barracudina, animals forming group 1 dominated in winter. Group 1 is formed of Arctic cod and herring with total lipid share of dry weight varying from 5.4 to 6.2% (**Table 3**). Arctic cod had high percentages (>10%) of 20:1(n-9) FA, as well as moderate concentrations (5-10%) of 22:1(n-11) and 20:5(n-3) FA (**Table 3**). Their proportion of 22:6(n-3) FA was higher in January (22%) than in August (12%). Arctic cod had low ratios of 22:1(n-9)/20:1(n-9) Falc (38%) (**Table 3**). Herring had high percentages of 22:6(n-3), 20:1(n-9) and 22:1(n-11) FA (**Table 2**).

Group 2 comprises *M. norvegica* and *T. libellula* (**Figure 5**), with total lipid concentrations varying from 9.1 to 15.6% of dry mass (**Table 3**). *Meganyctiphanes norvegica* had high percentages of 22:1(n-11) and 22:6(n-3) FA, as well as moderate concentrations of 16:1(n-7) and 20:5(n-3) FA. They also comprised a high ratio of 22:1/20:1 Falc (**Table 2**). *Themisto libellula* had moderate to high levels of 20:1(n-9) and 20:5(n-3) FA. They also had moderate amounts of 16:1(n-7), 18:4(n-3), 22:1(n-11) and 22:6(n-3) FA, as well as 22:1(n-11) and 20:1(n-9) Falc in the ratio 1.08 (**Table 2**).

Group 3 partly overlaps group 2 and comprises daubed shanny and glacier lanternfish (**Figure 5**). These species have high total lipid content: 18.2% (daubed shanny) and 33.4% (glacier lanternfish; **Table 3**) of dry mass. Daubed shanny had high percentages of 20:5(n-3) and 22:6(n-3) FA, moderate levels of 20:1(n-9) and 22:1(n-11) FA, very high levels of 20:1 and 22:1 Falc, and a 22:1(n-9)/20:1(n-9) Falc ratio of 2.10 (**Table 2**). Glacier lanternfish had high concentrations of 20:1(n-9) and 22:1(n-11) FA, as well as moderate percentages of 16:1(n-7), 20:5(n-3), and 22:6(n3) FA. They had a ratio 22:1(n-9)/20:1(n-9) of 1.86 (**Table 2**).

Group 4 is composed of redfish, the euphausiid *T. inermis* and spotted barracudina (**Figure 5**). Redfish had a total lipid content varying from 3% of dry mass in January to 10.5% in August. In contrast, *T. inermis* had a higher lipid content in January (22.2%) than in August (13.4%). Spotted barracudina had the higher concentration of lipids of all species (44.7% of dry mass in August) (**Table 3**). Beaked redfish had high concentrations of 20:5(n-3) and 22:6(n-3) FA. Spotted barracudina had high concentrations of 16:1(n-7) and 20:5(n-3) FA, and moderate levels of 22:6(n-3) FA. *Thysanoessa inermis* had high concentrations of 20:5(n-3) FA, as well as moderate levels of 16:1(n-7), 18:4(n-3), and 22:6(n-3) FA.

DISCUSSION

Seasonal Variations in Biomass and Assemblage of Macrozooplankton and Pelagic Fish

The Svalbard branch of AW inflow advected and concentrated zooplankton and fish species of boreal origin from the North Atlantic into the AW mass north of Svalbard. The Svalbard branch follows the slope between the 600–1000 m isobaths (Meyer et al., 2017) with currents ∼0.5 Sverdrup (Koenig et al., 2017). These isobaths correspond to the location where the AW thickened in January (**Figure 1B**). As most organisms followed the inflow of AW above the slope, in January the SSL was thicker and denser above the slope than above the colder and fresher deeper basin (**Figure 1C**). The strong intrusion of AW up to the surface above the slope likely explains the absence of ice in the study area (Polyakov et al., 2017).

The s_A values are proxies for the biomass of organisms within the SSL. The average s_A value in summer (351 m^2 nmi^{-2}) was more similar to values from boreal regions (e.g., 100-400 m^2 nmi^{-2} north west of the British Isles, 56°-60°N; Godø et al., 2009) than tropical and subtropical areas (mean of 1864 m^2 nmi^{-2} for the world's oceans between 40°S and 40°N; Irigoien et al., 2014). The SSL we detected in August was also weaker than SSL in the North Atlantic (e.g., 1165-1443 m^2 nmi^{-2} during daytime; Fennell and Rose, 2015). Our mean s_A value in August was slightly higher and our mean s_A values in January (56-57 m^2 nmi^{-2}) slightly lower than observations from the same area in August-September 2014 (66–240 m^2 nmi^{-2}; Knutsen et al., 2017), which supports our conclusion that the backscatter increases in summer, but also suggests interannual variations. Previous studies of SSL in the Barents Sea reported a decrease in backscatter from south to north [e.g., 215 to 81 m^2 nmi^{-2} (Siegelman-Charbit and Planque, 2016) and 365 to 66 m^2 nmi^{-2} (Knutsen et al., 2017)], which is consistent with our observations from January but not August. However, the latitudinal range we covered was smaller than in these studies and intraseasonal

TABLE 2 | Fatty acid and fatty alcohol (Alc) contents (in percent) within the most abundant fish and macrozooplankton species, including percentages of wax esters (WE).

Species	***Sebastes* sp.**		***Boreogadus saida***		***Themisto libellula***		***Leptoclinus maculatus***		***Thysanoessa inermis***		***Meganyctiphanes norvegica***		***Benthosema glaciale***		***Arctozenus risso***		***Clupea harrengus***	
Stations	**1597/74**		**1597/81**		**1597**		**1597**		**1608/74**		**1608/74**		**1608**		**1612**		**81**	
Fatty acids	**Mean**	***SD***	**Mean**	***SD***	**Mean**	***SD***	**Mean**	***SD***	**Mean**	***SD***	**Mean**	***SD***	**Mean**	***SD***	**Mean**	***SD***	**Mean**	***SD***
14:0	2.96	1.42	3.39	1.22	7.30	0.74	4.62	0.33	2.45	0.45	4.90	0.86	4.45	0.31	5.22	0.52	6.52	1.30
i-15:0	0.14	0.15	0.24	0.14	0.71	0.12	0.35	0.08	0.15	0.12	0.40	0.15	0.18	0.17	0.22	0.04	0.44	0.13
15:0	0.38	0.06	0.38	0.06	0.51	0.08	0.42	0.08	0.12	0.09	0.53	0.09	0.12	0.11	0.25	0.02	0.80	0.10
16:0	18.30	1.13	15.48	3.52	11.40	1.60	14.57	1.66	21.03	1.18	14.79	2.19	5.31	0.72	11.03	0.89	15.97	1.39
16:1(n-7)	4.37	1.95	6.43	4.37	6.96	1.00	4.93	0.59	7.28	2.42	5.29	1.31	9.57	0.60	11.25	0.58	4.81	1.02
16:1(n-5)	0.30	0.03	0.44	0.08	0.43	0.24	0.41	0.04	0.19	0.13	0.39	0.14	0.53	0.28	0.33	0.03	0.47	0.05
16:2(n-4)	0.45	0.03	0.54	0.05	0.28	0.16	0.48	0.08	0.60	0.29	0.27	0.11	0.74	0.04	0.68	0.02	0.52	0.03
16:3(n-4)	0.57	0.09	0.26	0.14	0.42	0.25	0.36	0.05	0.38	0.23	0.34	0.17	0.64	0.03	0.53	0.01	0.66	0.06
16:4(n-1)	0.39	0.31	0.19	0.18	0.38	0.24	0.34	0.07	0.65	0.31	0.09	0.12	0.73	0.39	0.44	0.03	0.00	0.00
18:0	5.17	1.13	2.51	0.91	1.14	0.31	2.07	0.21	2.16	0.85	1.76	0.39	0.83	0.77	0.61	0.10	1.92	0.63
18:1(n-9)	14.60	4.19	10.22	2.63	10.28	1.78	7.80	1.75	22.18	2.88	11.00	2.14	19.75	1.19	26.88	1.28	11.36	1.48
18:1(n-7)	3.51	0.59	2.75	0.78	2.00	0.48	1.90	0.27	9.19	1.53	4.13	0.75	2.05	0.21	5.72	0.65	2.14	0.43
18:1(n-5)	0.85	0.36	0.63	0.12	0.92	0.10	0.83	0.08	0.15	0.14	0.62	0.10	0.59	0.08	0.23	0.02	0.76	0.15
18:2(n-6)	1.55	0.16	1.63	0.85	3.98	0.43	2.02	0.64	1.56	0.44	1.73	0.38	1.57	0.12	1.98	0.13	1.29	0.16
18:3(n-6)	0.20	0.06	0.27	0.18	0.29	0.17	0.24	0.04	0.10	0.09	0.13	0.09	0.28	0.16	0.11	0.01	0.07	0.13
18:3(n-3)	0.58	0.21	0.69	0.18	1.21	0.25	1.01	0.13	0.86	0.33	0.72	0.27	1.18	0.09	1.06	0.04	0.90	0.33
18:4(n-3)	1.54	1.07	1.55	1.48	6.03	1.38	4.90	0.93	5.09	2.18	2.54	0.85	3.32	0.55	4.29	0.29	1.40	0.78
20:0	0.09	0.07	0.01	0.04	0.23	0.13	0.00	0.00	2.16	1.16	14.00	3.56	0.64	0.04	0.35	0.06	0.00	0.00
20:1(n-9)	4.06	1.11	12.87	5.37	12.05	1.19	8.75	4.83	0.28	0.17	0.63	0.17	12.19	0.66	2.18	0.71	11.46	2.27
20:1(n-7)	0.17	0.13	0.26	0.17	1.31	0.17	0.20	0.06	0.26	0.12	0.41	0.17	0.90	0.11	0.24	0.02	0.18	0.22
20:2(n-6)	0.33	0.37	0.32	0.22	0.74	0.16	0.36	0.09	0.02	0.05	0.00	0.00	0.15	0.13	0.17	0.00	0.22	0.32
20:4(n-6)	0.81	0.65	0.63	0.29	0.46	0.26	0.60	0.06	0.42	0.14	0.54	0.14	0.29	0.16	0.37	0.01	0.37	0.31
20:3(n-3)	0.01	0.04	0.03	0.05	0.19	0.11	0.00	0.00	0.04	0.06	0.09	0.15	0.21	0.20	0.20	0.08	0.00	0.00
20:4(n-3)	0.62	0.27	0.53	0.16	0.86	0.10	0.48	0.27	0.37	0.09	0.73	0.14	0.94	0.05	1.06	0.09	0.65	0.20
20:5(n-3)	10.84	1.48	8.98	1.93	11.46	1.58	14.49	2.02	13.82	2.62	9.30	1.57	6.09	1.07	11.59	0.54	5.70	0.41
22:1(n-11)	2.55	2.26	8.74	4.32	5.40	0.87	5.25	3.27	1.21	1.02	11.05	3.36	13.27	1.01	2.83	1.27	13.23	2.50
22:1(n-9)	0.58	0.16	1.34	0.49	0.92	0.07	0.67	0.29	0.31	0.17	1.24	0.31	1.40	0.24	0.62	0.10	0.86	0.14
22:1(n-7)	0.06	0.09	0.08	0.10	0.26	0.15	0.00	0.00	0.15	0.17	0.10	0.08	0.26	0.15	0.18	0.02	0.00	0.00
22:5(n-3)	0.76	0.15	0.72	0.16	0.65	0.17	0.71	0.14	0.12	0.09	0.59	0.08	0.71	0.09	0.75	0.12	0.77	0.02
22:6(n-3)	22.76	8.84	16.84	6.74	7.93	4.24	20.55	3.74	6.69	2.04	10.82	1.35	8.67	1.00	7.11	0.50	15.35	4.69
16:1(n-7)+ 20:5(n-3)	15.21	3.43	14.99	6.22	18.42	2.33	19.43	2.48	20.36	4.84	13.80	2.68	15.67	0.59	22.85	0.58	10.52	0.75
16:1(n-7/ 20:5(n-3)	0.4		0.72		0.61		0.34		0.53		0.57		1.63		0.97		0.85	

(Continued)

TABLE 2 | Continued

Species	*Sebastes* sp.		*Boreogadus saida*		*Themisto libellula*		*Leptoclinus maculatus*		*Thysanoessa inermis*		*Meganyctiphanes norvegica*		*Benthosema glaciale*		*Arctozenus risso*		*Clupea harrengus*	
Stations	1597/74		1597/81		1597		1597		1608/74		1608/74		1608		1612		81	
Fatty alcohols	Mean	SD			Mean	SD	Mean	SD			Mean	SD	Mean	SD	Mean	SD	Mean	SD
14:0Alc	26.26	19.66	16.83	30.00	4.21	0.60	10.55	9.09	27.49	5.56	33.37	13.93	6.88	0.93	9.06	1.71	8.94	17.88
16:0Alc	52.39	31.69	16.45	16.95	9.84	0.90	12.73	12.04	55.49	8.90	43.30	15.33	22.96	1.51	45.11	2.56	16.06	32.12
20:1Alc	4.04	7.66	33.11	21.28	37.78	1.87	23.60	6.59	2.33	2.80	0.88	2.91	18.48	1.20	8.89	2.42		
22:1Alc	4.95	9.78	12.46	18.43	40.87	2.42	49.66	18.49	2.61	3.95	10.88	18.20	34.52	2.72	9.19	2.34		
22:1/20:1Alc	1.23		0.38		1.08		2.10		1.91		18.8		1.86		1.03			
WE-%	1.81	1.07	3.12	1.37	36.50	7.54	12.67	9.28	30.41	4.67	2.0	1.88	79.19	2.48	56.91	4.20	0.48	0.66

Only fatty acids and alcohols present in at least one species are listed.

variations might have been dominated by the shelf-basin gradient rather than a south-north gradient.

Calculating the biomass of mesopelagic organisms within SSL imposes several caveats and uncertainties. Biomass estimates from acoustic data are based on the species assemblage as well as average size and weight of each species in net samples. Midwater trawl nets, such as the Harstad trawl, are selective and do not sample the whole community (De Robertis et al., 2017). Despite a 10 mm-mesh in the codend, some of the smaller organisms might have passed through the large meshes of several cm in the first parts of the net. On the other hand, larger fish avoid nets more easily than smaller ones. Hence, net selectivity could have positively or negatively biased our estimates and a larger net with smaller mesh at the mouth would have made the catch more representative of the actual community. Midwater trawls are inefficient at sampling siphonophores because these fragile organisms are easily destroyed. Only one siphonophore was sampled in January 2016, but their abundance was likely higher as they can be abundant at high latitudes (Knutsen et al., 2018). Siphonophores have gas-filled pneumatophores that resonate at similar frequencies as swimbladdered fish, and it is possible that some of the signal classified as fish was in fact coming from siphonophores, thus resulting in an overestimation of the fish biomass. In other areas where SSL are mainly composed of Myctophidae with swimbladder characteristics changing with ontogeny and depth (i.e., changes in occurrence, shape, and composition of the swimbladder), variations in their TS-length relationship greatly complicate biomass calculations (Yasuma et al., 2010). Here, however, this bias was likely limited as Myctophidae only represented 2% or less of the biomass (**Table 1**). In addition to net selectivity, TS dependency on depth and non-linearity in EK60 power measurements at lower SNR prevailing at mesopelagic depths may have biased biomass estimates either way.

Most caveats and biases were likely similar from one season to the other, and viewing our biomass estimates as relative rather than absolute values should not affect the interpretation and conclusions. Despite high uncertainties, these estimates provide rare quantification of seasonal variations in mesopelagic biomass in the high Arctic, which can be used as a baseline from which to monitor future changes in the pelagic ecosystem. They also demonstrate that macrozooplankton provided most of the biomass and lipids available within the SSL in summer, and that their biomass diminished by one order of magnitude in winter. Hence, macrozooplankton should be included in future surveys quantifying mesopelagic ecosystems.

The species assemblage varied more seasonally than spatially and, in contrast with many oceanographic regions (Irigoien et al., 2014), Myctophidae did not dominate the mesopelagic fish assemblage (**Table 1**). The assemblage in August was significantly different from the assemblages in January, which were relatively consistent between January 2016 and 2017 (**Figure 4**). In August, macrozooplankton such as the amphipod *T. libellula*, the euphausiid *M. norvegica*, and the medusa *C. capillata* dominated the biomass. The high biomass of macrozooplankton and jellyfish and the occurrence of juvenile redfish, spotted barracudina, and some glacier lanternfish is consistent with previous observations

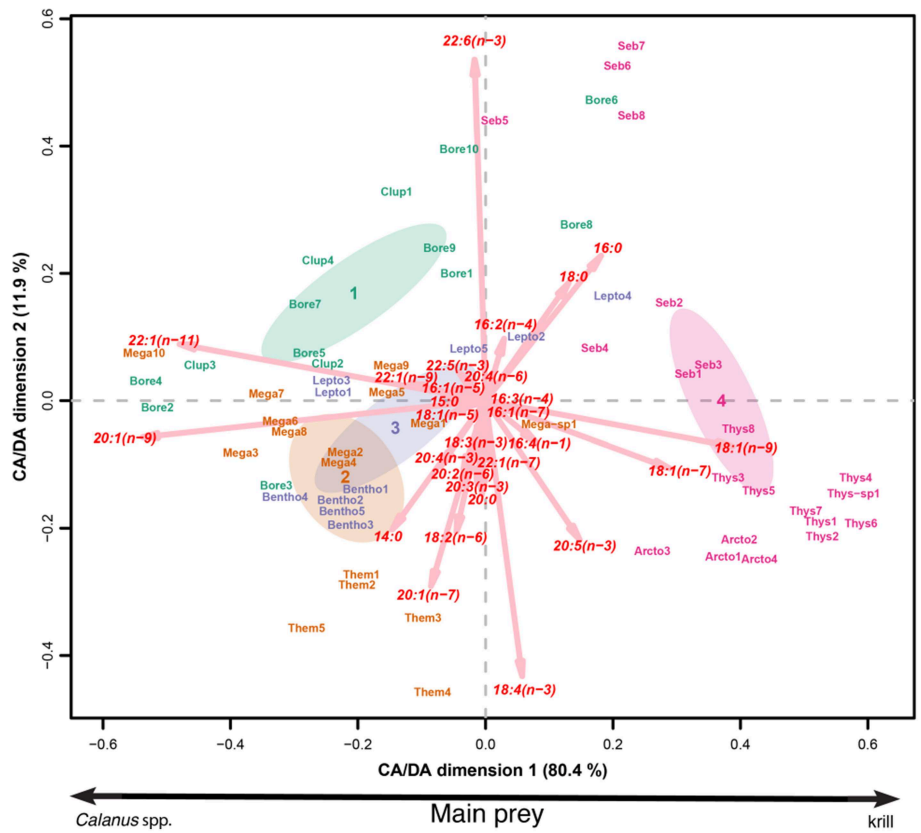

FIGURE 5 | Ordination plot of the CA/DA conducted on the concentration (%) of FATM for each individual organism. Bore corresponds to *Boreogadus saida*, Clup to *Clupea harengus*, Them to *Themisto libellula*, Mega to *Meganyctiphanes norvegica*, Lepto to *Leptoclinus maculatus*, Bentho to *Benthosema glaciale*, Seb to *Sebastes mentella*, Thys to *Thysanoessa inermis*, and Arcto to *Arctozenus risso*.

of the SSL north of Svalbard (Gjøsæter et al., 2017; Knutsen et al., 2017). However, in contrast with these studies which mainly sampled Atlantic fish species, Arctic cod dominated the biomass of pelagic fish in August (45%). The relatively high abundance of Arctic cod among Atlantic species is not surprising as the species is abundant in the northern Barents Sea where its distribution overlaps with that of Atlantic cod and haddock (Renaud et al., 2012), as well as that of juvenile redfish (Eriksen et al., 2015). Year class strength of Arctic cod is highly variable, and since mainly age-0 and age-1 individuals occupied the SSL, the biomass of pelagic Arctic cod likely varies considerably from year to year.

Cyanea capillata and *T. inermis* dominated the macrozooplankton assemblage in January (*G. fabricii* were also abundant in January 2017), and juvenile beaked redfish dominated the pelagic fish assemblage (>83% of the biomass). Arctic cod only represented <2% of the biomass in January. Arctic cod sometimes remain under sea ice in the high Arctic (Lønne and Gulliksen, 1989), but no ice-associated Arctic cod were sampled nor observed acoustically in the same region in June 2017 (Pierre Priou, Memorial University, unpublished data). The average length of Arctic cod in winter (<10 cm) suggests that they were part of the age-1 cohort (Lønne and Gulliksen, 1989). Age-1 Arctic cod can be sexually mature (Nahrgang et al., 2014) and winter spawning migrations toward spawning areas in the fjords of Svalbard and the eastern Barents Sea (Ajiad et al., 2011) could explain the near absence of Arctic cod in January. Another plausible explanation is a change in preferred habitat with ontogenetic development, because Arctic cod leave their pelagic habitat for the demersal zone as they grow (Geoffroy et al., 2016).

The photoperiod constraint hypothesis suggests that inferior feeding conditions imposed by the extremely low irradiance prevailing during the polar night limit the abundance and northward range expansion of pelagic fishes of boreal origin and their zooplankton prey into the high Arctic (Kaartvedt, 2008). Here, however, the lower biomass in winter might be related to other factors than the inability to forage during the polar night. We observed a large decrease in the biomass of macrozooplankton and fish in January, but for species of both boreal and Arctic origins. Zooplankton and juvenile pelagic fish from the North Atlantic are more likely to be advected northwards in summer, when they colonize the pelagic realm, than in winter when they descend at greater depths. This most likely contributes to the lower biomass in January. Furthermore, the decrease in fish biodiversity mostly results from

TABLE 3 | Mean dry weight, lipid weight and lipid/dry weight ratios with standard deviation (SD) for the most abundant fish and crustaceans.

Species and season	Dry weight (mg)		Total lipids (mg)		% total lipids/dry weight	
	Mean	SD	Mean	SD	Mean	SD
Sebastes mentella (January)	344.3	114.7	11.1	3.3	3.0	0.8
Sebastes mentella (August)	147.6	40.9	15.4	6.4	10.5	1
Boreogadus saida (January)	285.5	110.7	17.9	9.8	6.0	2.1
Boreogadus saida (August)	582.8	610.4	18.4	15.5	5.4	4.4
Leptoclinus maculatus (August)	125.9	58.0	21.5	7.5	18.2	4.9
Benthosema glaciale (August)	215.4	75.9	72.2	29.7	33.4	9.9
Arctozenus risso (August)	11,574.5	3,724.6	2,596.1	2,067.3	44.7	8.9
Clupea harrengus (January)	627.0	232.2	41.6	22.2	6.2	1.8
Themisto libellula (August)	156.0	37.0	12.7	4.6	9.1	5.1
Thysanoessa inermis (January)	20.1	12.9	5.1	4.5	22.2	7.5
Thysanoessa inermis (August)	145.7	125.1	15.0	8.1	13.4	8.6
Meganyctiphanes norvegica (January)	53.4	43.8	9.7	10.2	15.6	4.6
Meganyctiphanes norvegica (August)	127.9	46.3	11.8	0.04	10.4	4.4

N = 5 for each species/season.

the ontogenetic descent at depth of benthic and demersal species. For instance, the wolffish caught in August were age-0 juveniles with a mean length of 6.29 cm, a length at which they descend to demersal depths before becoming exclusively benthic once they reach 10 cm (Moksness and Pavlov, 1996). Similarly, the mean lengths of the juvenile Atlantic cod and haddock caught in August indicate that they were on the verge of quitting the pelagic realm (Lough et al., 1989; Lomond, 1998). Most of these gadids likely descended to demersal depths by January, which explains their lower biomass in winter despite the presence of relatively warm AW. Although some pelagic boreal species might not survive the polar night, the only species for which we might infer such a phenomenon is the spotted barracudina, which remains pelagic at the adult stage and was absent in January. Juvenile beaked redfish, another boreal fish, displayed relatively constant biomass between seasons (**Figure 3**). The polar night may thus restrict the northward range expansion of some species, such as spotted barracudina, but others such as the beaked redfish can survive the extreme conditions prevailing during the high Arctic winter.

Hollowed et al. (2013) predicted a northward range expansion of beaked redfish in the Arctic Ocean. Until the 1990s, juvenile Arctic cod dominated the fall pelagic fish assemblage in the offshore region of western Svalbard. Since then, juvenile redfish have become the dominant species because of high recruitment events, the northward retreat of the ice edge, and a longer ice-free season resulting in surface temperatures reaching 2-5.5°C (Hollowed et al., 2013; Eriksen et al., 2015). Here, we demonstrate that juvenile redfish can also dominate the northern Barents Sea pelagic assemblage in winter. In the Barents and Norwegian Seas, the ovoviviparous beaked redfish spawn in fall and larval extrusion occurs in March-April (Drevetnyak and Nedreaas, 2009; Planque et al., 2013). Based on an average flow of 0.1 m s^{-1} within the West Spitsbergen Current (Fahrbach et al., 2001; Cokelet et al., 2008), redfish captured on 28 August would have taken 96 days to drift the 830 km between their northernmost known extrusion zone close to Bjørnøya (Hollowed et al., 2013) and the northernmost sampling station, which implies an extrusion date prior to 24 May. The abundant age-0 redfish sampled up to 81.4°N in August could thus have hatched in their known larval extrusion zone above the continental shelf break in the Barents and Norwegian Seas (Planque et al., 2013). Hence, for the moment, high abundances of age-0 redfish this far north does not necessarily imply a northward expansion of the extrusion zone. However, it suggests that they can survive and grow (e.g., mean length of 4 cm in August and 6 cm in January) after being advected into the Arctic.

Seasonal Changes in Trophic Relationships

Although most species, and particularly Arctic cod, have a varied diet that changes with their size and habitat (Cusa, 2016), two pelagic food webs prevailed. The first one was based on *Calanus* spp. (indicated by the 20:1(n-9) and 22:1(n-11) FA; **Supplementary Table 4**) and the second was based on krill (*Thysanoessa* spp.). These food webs are contrasted in **Figure 5**, where spotted barracudina and redfish are part of the krill-based food web (group 4) and *T. libellula*, *M. norvegica*, age-1 Arctic cod, herring, daubed shanny, and glacier lanternfish mainly prey on *Calanus* spp. (groups 1-3). Moreover, the high 22:1/20:1 Falc ratios of *M. norvegica*, glacier lanternfish and daubed shanny indicate that these taxa mainly fed on *C. hyperboreus*, while *T. libellula* and Arctic cod rather preyed on *C. finmarchicus* and *C. glacialis* (Falk-Petersen et al., 1987; Graeve et al., 1994, 1997). Similarly, Petursdottir et al. (2008) demonstrated that beaked redfish in the Reykjanes Ridge (Iceland) fed predominantly on krill, while daubed shanny from Ullsfjorden (70°N, Norway) fed on *C. hyperboreus* (Falk-Petersen et al., 1986). *Themisto libellula* in the Fram Strait (Auel et al., 2002) and off East Greenland (Kraft et al., 2015) also rely on *C. finmarchicus* as their main prey.

Arctic cod, *T. libellula*, and *M. norvegica* dominated the fish/crustacean assemblage in August, while redfish and *Thysanoessa inermis* dominated in January. Hence, we conclude

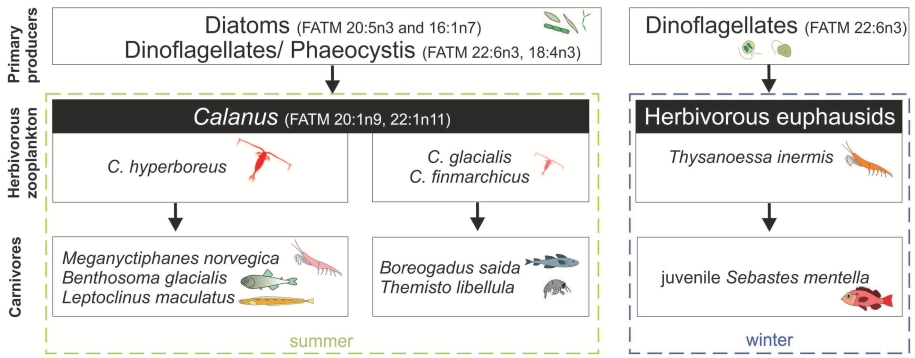

FIGURE 6 | Simplified schematic of the main pelagic food web pathways in summer 2016 and winters 2016-2017 based on the FATM analysis.

to a switch from a *Calanus*-based pelagic food web in summer to a krill-based pelagic food web in winter (**Figure 6**). This switch also explains why the few Arctic cod sampled in January fed more on krill than those sampled in August (Bore 6–10 vs. Bore 1–5; **Figure 5**). In the Arctic, primary production diminishes drastically after the spring bloom and the algal community changes from an abundance of diatoms in spring to a domination of flagellates in winter (van Leeuwe et al., 2018). Our sampling was conducted in August and January, after the spring bloom, which explains why most species contained relatively high concentrations of the flagellate marker 22:6(n-3) FA (Ackman et al., 1968) and why the concentrations of this marker doubled in Arctic cod and redfish between August and January. Despite lower algal abundance and a dominance by flagellates in winter (van Leeuwe et al., 2018), *T. inermis* likely continued to feed during that period as their total lipid/dry weight ratio slightly increased in winter (from 13% to 22%; **Table 3**). Huenerlage et al. (2015) concluded that lipid reserves in *T. inermis* are not sufficient to survive the Arctic winter without feeding and suggested that they shift to an opportunistic feeding mode during that season. A shift to detridal and benthic food sources during winter has also been suggested for *Thysanoessa raschii* (Sargent and Falk-Petersen, 1981). The ability to feed in winter may explain why *Thysanoessa* spp. dominated the macrozooplankton assemblage in January. In turn, their high biomass supported the juvenile redfish population in winter (**Figure 3**).

In August, *Calanus* spp. had started their descent to overwintering depths and were distributed throughout the water column down to 800 m, with a WMD of 408 m (M. Daase, unpublished data). They were thus accessible to Arctic cod, *T. libellula* and *M. norvegica,* distributed at similar depths, especially as these visual predators are adapted to the low light levels prevailing at these depths (Jönsson et al., 2014; Cohen et al., 2015). Surprisingly, the herbivorous *Thysanoessa* spp. were also located between 200 m and 700 m in August, below the productive euphotic zone. This behavior might be due to avoidance of visual predators, such as seabirds, in the top 200 m after the spring bloom, when irradiance increases and primary production diminishes.

In January, *C. finmarchicus* overwinters below the AW in the North Atlantic and Greenland Sea, and thus out of range for pelagic fish and zooplankton (Hirche, 1991; Gaardsted et al., 2010). However, in the waters north and west of Svalbard *C. finmarchicus* has recently been observed to concentrate in the upper 50 m in January (Daase et al., 2014; Berge et al., 2015; Basedow et al., 2018), an observation that has a great impact on estimates of the amount of *C. finmarchicus* advected in the Arctic with AW (Basedow et al., 2018). *Calanus* abundance integrated over the water column was, however, 5-10 times lower in January than in August (11,500-28,300 ind. m^{-2} and 111,640 ind. m^{-2}, respectively; Daase, unpublished data). Hence, *Calanus* spp. were less available for pelagic predators in January compared to August. In contrast, euphausiids and juvenile redfish remained abundant between 50 m and 500 m in winter, where they supported the winter krill-based food web (**Figure 6**). As AW progresses further east into the Eurasian Basin since the last decades (Polyakov et al., 2017), it is possible that more krill and redfish are advected in the European Arctic and that the krill-based food web becomes increasingly important in the region. Interestingly, Einarson (1945) showed that krill was also abundant in Svalbard waters during the last warm period in the 1930s.

CONCLUSIONS

This study provides rare information on the seasonal variations in biomass and composition of pelagic fish and macrozooplankton in the high Arctic. It shows that the diversity and total biomass of pelagic species forming the SSL diminishes during the polar night. Part of this decrease might be related to ontogenetic migrations toward the seafloor. Yet, some pelagic Atlantic-taxa such as the spotted barracudina could be on a trail to death when advected with AW into the high Arctic. Others like juvenile beaked redfish thrive during the polar night, possibly because they can exploit the lipid-rich krill-based food web prevailing during this period. Redfish have strong year classes followed by years with very low recruitment (Drevetnyak and Nedreaas, 2009). Future surveys

should continue to monitor the fate of the strong 2016-2017 cohorts advected into the high Arctic to verify if they settle and reproduce in the region or if they migrate back south to their known spawning grounds. Despite a decrease in biomass during winter, pelagic fish and macrozooplankton advected in the high Arctic form a lipid-rich SSL which represents an important source of energy for the whales and other top predators spending the summer and fall north of Svalbard (Falk-Petersen et al., 2009a; Haug et al., 2017).

DATA AVAILABILITY

The datasets generated for this study are available on request to the corresponding author.

ETHICS STATEMENT

All applicable international, national, and/or institutional guidelines for the care and use of animals were followed. This study was carried out with permission from the Governor on Svalbard and followed the strict regulations regarding health, environment and safety enforced at UNIS and UiT.

AUTHOR CONTRIBUTIONS

MGe designed the study and led sampling activities, analyses of the acoustic datasets, and writing of the manuscript. MD, MC, and NS contributed to sampling activities and analyses of the zooplankton and acoustic datasets. GD led species assemblage analyses. MGr conducted lipid analyses. FC contributed to interpret the physical oceanography results. JB, PR, and SF-P contributed to design the study and participated in sampling activities. All co-authors contributed to writing and reviewing the manuscript.

FUNDING

This study was supported by the Research Council of Norway (NFR) through the Arctic ABC project #244319 and the Marine Night project #226417. It is a contribution toward the ARCTOS research network (https://arctos.uit.no/), the Arctic Science Partnership (www.asp.org), and the Ocean Frontier Institute (oceanfrontierinstitute.com) funded through Canada's First Research Excellence Fund.

ACKNOWLEDGMENTS

We thank the officers and crew of the R/V *Helmer Hanssen* and the numerous colleagues who helped during sampling. Special thanks to Carl Ballantine, Sam Newby, Julia Gossa, and Paul Dubourg for their contribution to trawl sampling in January 2016 and to Bodil Bluhm who was chief scientist in January 2017. We thank the students of the University Centre in Svalbard (UNIS) course AB-320 who contributed to sampling in August 2016. Thanks to Arild Sundfjord who provided valuable knowledge about the inflow of AW in the Arctic.

SUPPLEMENTARY MATERIAL

The Supplementary Material for this article can be found online at: https://www.frontiersin.org/articles/10.3389/fmars.2019.00364/full#supplementary-material

REFERENCES

Ackman, R. G., Tocher, C. S., and McLachlan, J. (1968). Marine phytoplankter fatty acids. *J. Fish. Res. Board. Can.* 25, 1603–1620.

Ajiad, A., Oganin, I. A., and Gjøsæter, H. (2011). "Polar cod," in *The Barents Sea Ecosystem: Russian-Norwegian Cooperation in Science and Management*, ed. T. Jakobsen, and V. Ozhigin (Trondheim: Tapir Academic Press), 315–328.

Aksnes, D. L., Røstad, A., Kaartvedt, S., Martinez, U., Duarte, C. M., and Irigoien, X. (2017). Light penetration structures the deep acoustic scattering layers in the global ocean. *Sci. Adv.* 3:e1602468. doi: 10.1126/sciadv.1602468

Auel, H., Harjes, M., da Rocha, R., Stubing, D., and Hagen, W. (2002). Lipid biomarkers indicate different ecological niches and trophic relationships of the Arctic hyperiid amphipods *Themisto abyssorum* and *T. libellula*. *Polar Biol.* 25, 374–383. doi: 10.1007/s00300-001-0354-7

Aumont, O., Maury, O., Lefort, S., and Bopp, L. (2018). Evaluating the potential impacts of the diurnal vertical migration by marine organisms on marine biogeochemistry. *Glob. Biogeochem. Cycles* 32, 1622–1643. doi: 10.1029/2018GB005886

Basedow, S. L., Sundfjord, A., von Appen, W. J., Halvorsen, E., Kwasniewski, S., and Reigstad, M. (2018). Seasonal variation in transport of zooplankton into the Arctic basin through the Atlantic gateway, Fram Strait. *Front. Mar. Sci.* 5:194. doi: 10.3389/fmars.2018.00194

Benoit, D., Simard, Y., and Fortier, L. (2008). Hydroacoustic detection of large winter aggregations of Arctic cod (*Boreogadus saida*) at depth in ice-covered Franklin Bay (Beaufort Sea). *J. Geophys. Res. Ocean.* 113, C06S90. doi: 10.1029/2007JC004276

Benoit-Bird, K. J., and Au, W. W. L. (2004). Diel migration dynamics of an island-associated sound-scattering layer. *Deep-Sea Res. Part I.* 51, 707–719. doi: 10.1016/j.dsr.2004.01.004

Berge, J., Daase, M., Renaud, P, E., Ambrose, W., G. Jr., Darnis, G., Last, K., S., et al. (2015). Unexpected levels of biological activity during the polar night offer new perspectives on a warming Arctic. *Curr. Biol.* 25, 2555–2561. doi: 10.1016/j.cub.2015.08.024

Cohen, J. H., Berge, J., Moline, M. A., Sørensen, A. J., Last, K., Falk-Petersen, S., et al. (2015). Is ambient light during the high Arctic polar night sufficient to act as a visual cue for zooplankton? *PLoS ONE.* 10:e0126247. doi: 10.1371.journal.pone.0126247

Cokelet, E. D., Tervalon, N., and Bellingham, J. G. (2008). Hydrography of the West spitsbergen current, svalbard branch: autumn 2001. *J. Geophys. Res. Ocean.* 113:C01006. doi: 10.1029/2007JC004150

Crawford, R. E. (2016). Occurrence of a gelatinous predator (*Cyanea capillata*) may affect the distribution of *Boreogadus saida*, a key Arctic prey fish species. *Polar Biol.* 39, 1049–1055. doi: 10.1007/s00300-015-1779-8

Cusa, M. (2016). *The effect of seasonality on polar cod (Boreogadus saida) dietary habits and temporal feeding strategies in Svalbard waters* (Master's thesis). Tromsø: UiT The Arctic University of Norway

Daase, M., Varpe, Ø., and Falk-Petersen, S. (2014). Non-consumptive mortality in copepods: occurrence of *Calanus* spp. carcasses in the Arctic ocean during winter. *J. Plankt. Res.* 36, 129–144. doi: 10.1093/plankt/fbt079

Dale, T., Bagoien, E., Melle, W., and Kaartvedt, S. (1999). Can predator avoidance explain varying overwintering depth of *Calanus* in different oceanic water masses? *Mar. Ecol. Prog. Ser.* 179, 113–121. doi: 10.3354/meps179113

Dalsgaard, J., St. John, M., Kattner, G., Müller-Navarra, D., and Hagen, W. (2003). Fatty acid trophic markers in the pelagic marine environment. *Adv. Mar. Biol.* 46, 225–340. doi: 10.1016/S0065-2881(03)46005-7

Darnis, G., Barber, D. G., and Fortier, L. (2008). Sea ice and the onshore-offshore gradient in pre-winter zooplankton assemblages in southeastern Beaufort Sea. *J. Mar. Syst.* 74, 994–1011. doi: 10.1016/j.jmarsys.2007.09.003

De Robertis, A., and Higginbottom, I. (2007). A post-processing technique to estimate the signal-to-noise ratio and remove echosounder background noise. *ICES J. Mar. Sci.* 64, 1282–1291. doi: 10.1093/icesjms/fsm112

De Robertis, A., McKelvey, D. R., and Ressler, P. H. (2010). Development and application of an empirical multifrequency method for backscatter classification. *Can. J. Fish. Aquat. Sci.* 67, 1459–1474. doi: 10.1139/F10-075

De Robertis, A., Taylor, K., Williams, K., and Wilson, C. D. (2017). Species and size selectivity of two midwater trawls used in an acoustic survey of the Alaska Arctic. *Deep Sea Res. Part II*. 135, 40–50. doi: 10.1016/j.dsr2.2015.11.014

D'Elia, M., Warren, J. D., Rodriguez-Pinto, I., Sutton, T. T., Cook, A., and Boswell, K. M. (2016). Diel variation in the vertical distribution of deep-water scattering layers in the Gulf of Mexico. *Deep-Sea Res. Part I*. 115, 91–102. doi: 10.1016/j.dsr.2016.05.014

Demer, D. A., Berger, L., Bernasconi, M., Bethke, E., Boswell, K., Chu, D., et al. (2015). *Calibration of Acoustic Instruments*. International Council for the Exploration of the Sea (ICES) Cooperative Research Report No. 326.

Drevetnyak, K., and Nedreaas, K. H. (2009). Historical movement pattern of juvenile beaked redfish (Sebastes mentella Travin) in the Barents Sea as inferred from long-term research survey series. *Mar. Biol. Res.* 5, 86–100. doi: 10.1080/17451000802534865

Einarson, H. (1945). *Euphausiacea. 1. North Atlantic species*. Dana Report. 27, 1–185.

Eriksen, E., Ingvaldsen, R. B., Nedreaas, K., and Prozorkevich, D. (2015). The effect of recent warming on polar cod and beaked redfish juveniles in the Barents Sea. *Regional Stud. Mar. Sci.* 2, 105–112. doi: 10.1016/j.rsma.2015.09.001

Fahrbach, E., Meincke, J., Osterhus, S., Rohardt, G., Schauer, U., Tverberg, V., et al. (2001). Direct measurements of volume transports through Fram Strait. *Polar Res.* 20, 217–224. doi: 10.1111/j.1751-8369.2001.tb00059.x

Falk-Petersen, I. B., Falk-Petersen, S., and Sargent, J. (1986). Nature, origin and possible roles of lipid deposits in *Maurolicus muelleri* (Gmelin) and *Bentosema glaciale* (Reinhart) from Ullsfjorden, Northern Norway. *Polar Biol.* 5, 235–240.

Falk-Petersen, S., Haug, T., Hop, H., Nilssen, K. T., and Wold, A. (2009a). Transfer of lipids from plankton to blubber of harp and hooded seals off East Greenland. *Deep-Sea Res. Part II*. 56, 2080–2086. doi: 10.1016/j.dsr2.2008.11.020

Falk-Petersen, S., Mayzaud, P., Kattner, G., and Sargent, J. (2009b). Lipids and life strategy of Arctic *Calanus*. *Mar. Biol. Res.* 5, 18–39. doi: 10.1080/17451000802512267

Falk-Petersen, S., Sargent, J., and Tande, K. S. (1987). Lipid composition of zooplankton in relation to the sub-Arctic food web. *Polar Biol.* 8, 115–120.

Falk-Petersen, S., Sargent, J. R., and Hopkins, C. C. E. (1990). "Trophic relationships in the pelagic arctic food web," in *Trophic Relationships in the Marine Environment*, eds. M. Barnes and R. N. Gibson (Aberdeen: Scotland University Press), 315–333.

Falk-Petersen, S., Timofeev, S., Pavlov, V., and Sargent, J. R. (2007). "Climate variability and possible effect on arctic food chains. The role of Calanus," in *Arctic-Alpine Ecosystems and People in a Changing Environment*, eds. J. B. Ørbæk, T. Tombre, R. Kallenborn, E. Hegseth, S. Falk-Petersen, and A. H. Hoel (Berlin: Springer Verlag), 147–166.

Fennell, S., and Rose, G. (2015). Oceanographic influences on deep scattering layers across the North Atlantic. *Deep-Sea Res. Part I*. 105, 132–141. doi: 10.1016/j.dsr.2015.09.002

Foote, K. G. (1987). Fish target strengths for use in echo integrator surveys. *J. Acoust. Soc. Am.* 82, 981–987. doi: 10.1121/1.395298

Fossheim, M., Primicerio, R., Johannesen, E., Ingvaldsen, R. B., Aschan, M. M., and Dolgov, A. V. (2015). Recent warming leads to a rapid borealization of fish communities in the Arctic. *Nat. Clim. Change.* 5, 673–677. doi: 10.1038/NCLIMATE2647

Francois, R. E., and Garrison, G. R. (1982). Sound absorption based on ocean measurements. Part II: Boric acid contribution and equation for total absorption. *J. Acoust. Soc. Am.* 72, 1879–1890. doi: 10.1121/1.388673

Gaardsted, F., Zhou, M., Pavlov, V., Morozov, A., and Tande, K. S. (2010). Mesoscale distribution and advection of overwintering *Calanus finmarchicus* off the shelf of northern Norway. *Deep-Sea Res. Part I*. 57, 1465–1473. doi: 10.1016/j.dsr.2010.07.003

Gauthier, S., and Horne, J. K. (2004). Potential acoustic discrimination within boreal fish assemblages. *ICES J. Mar. Sci.* 61, 836–845. doi: 10.1016/j.icesjms.2004.03.033

Gauthier, S., and Rose, G. A. (2002). *In situ* target strength studies on Atlantic redfish (*Sebastes* spp.). *ICES J. Mar. Sci.* 59, 805–815. doi: 10.1006/jmsc.2002.1248

Geoffroy, M., Majewski, A., LeBlanc, M., Gauthier, S., Walkusz, W., Reist, J. D., et al. (2016). Vertical segregation of age-0 and age-1+ polar cod (*Boreogadus saida*) over the annual cycle in the Canadian Beaufort Sea. *Polar Biol.* 39, 1023–1037. doi: 10.1007/s00300-015-1811-z

Gjøsæter, H., Wiebe, P. H., Knutsen, T., and Ingvaldsen, R. B. (2017). Evidence of diel vertical migration of mesopelagic sound-scattering organisms in the Arctic. *Front. Mar. Sci.* 4:332. doi: 10.3389/fmars.2017.00332

Godø, O. R., Patel, R., and Pedersen, G. (2009). Diel migration and swimbladder resonance of small fish: some implications for analyses of multifrequency echo data. *ICES J. Mar. Sci.* 66, 1143–1148. doi: 10.1093./icesjms/fsp098

Graeve, M., Kattner, G., and Hagen, W. (1994). Diet induced changes in the fatty acid composition of arctic herbivorous copepods- experimental evidence of trophic markers. *J. Exp. Mar. Biol. Ecol.* 182, 97–110. doi: 10.1016/0022-0981(94)90213-5

Graeve, M., Kattner, G., and Piepenburg, D. (1997). Lipids in Arctic benthos: Does the fatty acid and alcohol composition reflect feeding and trophic interactions? *Polar Biol.* 18, 53–61. doi: 10.1007/s003000050158

Greenacre, M. J. (2016). *Correspondence Analysis in Practice*. Boca Raton: Chapman and Hall

Haug, T., Bogstad, B., Chierici, M., Gjøsæter, H., Hallfredsson, E. H., Høines, Å. S., et al. (2017). Future harvest of living resources in the Arctic Ocean north of the Nordic and Barents Seas: a review of possibilities and constraints. *Fish Res.* 188, 38–57. doi: 10.1016/j.fishres.2016.12.002

Hirche, H. J. (1991). Distribution of dominant calanoid copepod species in the Greenland Sea during late fall. *Polar Biol.* 11, 351–362.

Hollowed, A. B., Planque, B., and Loeng, H. (2013). Potential movement of fish and shellfish stocks from the sub-Arctic to the Arctic Ocean. *Fish Oceanogr.* 22, 355–370. doi: 10.1111/fog.12027

Huenerlage, K., Graeve, M., Buchholz, C., and Buchholz, F. (2015). The other krill: overwintering physiology of adult *Thysanoessa inermis* (Euphausiacea) from the hig-Arctic Kongsfjord. *Aquat. Biol.* 23, 225–235. doi: 10.3354/ab00622

Irigoien, X., Klevjer, T. A., Røstad, A., Martinez, U., Boyra, G., Acuña, J. L., et al. (2014). Large mesopelagic fishes biomass and trophic efficiency in the open ocean. *Nat. Commun.* 5:3271. doi: 10.1038/ncomms4271

Jarvis, T., Kelly, N., Kawaguchi, S., van Wijk, E., and Nicol, S. (2010). Acoustic characterisation of the broad-scale distribution and abundance of Antarctic krill (*Euphausia superba*) off East Antarctica (30-80°E) in January-March 2006. *Deep-Sea Res. Part II*. 57, 916–933. doi: 10.1016/j.dsr2.2008.06.013

Jönsson, M., Varpe, Ø., Kozłowski, T., Berge, J., and Kröger, R. H. (2014). Differences in lens optical plasticity in two gadoid fishes meeting in the Arctic. *J. Comp. Physiol. A*. 200, 949–957. doi: 10.1007/s00359-014-0941-z

Kaartvedt, S. (2008). Photoperiod may constrain the effect of global warming in arctic marine systems. *J. Plankt. Res.* 30, 1203–1206. doi: 10.1093/plankt/fbn075

Kattner, G., and Fricke, H. S. G. (1986). Simple gas-liquid chromatographic method for the simultaneous determination of fatty acids and alcohols in wax esters of marine organisms. *J. Chromatogr.* 361, 263–268.

Knutsen, T., Hosia, A., Falkenhaug, T., Skern-Mauritzen, R., Wiebe, P. H., Larsen, R. B., et al. (2018). Coincident mass occurrence of gelatinous zooplankton in Northern Norway. *Front. Mar. Sci.* 5:158. doi: 10.3389/fmars.2018.00158

Knutsen, T., Wiebe, P. H., Gjøsæter, H., Ingvaldsen, R. B., and Lien, G. (2017). High latitude epipelagic and mesopelagic scattering layers - a reference for future Arctic ecosystem change. *Front. Mar. Sci.* 4:334. doi: 10.3389/fmars.2017.00334

Koenig, Z., Provost, C., Sennéchael, N., Garric, G., and Gascard, J. C. (2017). The yermak pass branch: a major pathway for the Atlantic water North of Svalbard? *J. Geophys. Res. Ocean.* 122, 9332–9349. doi: 10.1002/2017JC013271

Korneliussen, R. J., Berger, L., Campanlla, F., Chu, D., Demer, D., De Robertis, A., et al. (2018). *Acoustic Target Classification*. International Council for the Exploration of the Sea (ICES) Cooperative Research Report No. 344.

Kraft, A., Graeve, M., Janssen, D., Greenacre, M., and Falk-Petersen, S. (2015). Arctic pelagic amphipods: lipid dynamics and life strategy. *J. Plankt. Res.* 37:790–807. doi: 10.1093/plankt/fbv052

Lomond, T. M. (1998). Transition from pelagic to benthic prey for age group 0-1 Atlantic cod. *Fish. Bull.* 96, 908–911.

Lønne, O. J., and Gulliksen, B. (1989). Size, age and diet of polar cod, *Boreogadus saida* (Lepechin 1773) in ice covered waters. *Polar Biol.* 9, 187–191.

Lough, R. G., Valentine, P. C., Potter, D. C., Auditore, P. J., Bolz, G. R., Neilson, J. D., et al. (1989). Ecology and distribution of juvenile cod and haddock in relation to sediment type and bottom currents on eastern Georges Bank. *Mar. Ecol. Prog. Ser.* 56, 1–12.

Mackenzie, K. V. (1981). Nine-term equation for sound speed in the oceans. *J. Acoust. Soc. Am.* 70:807–812. doi: 10.1121/1.386920

Meyer, A., Fer, I., Sundfjord, A., and Peterson, A. K. (2017). Mixing rates and vertical heat fluxes north of Svalbard from Arctic winter to spring. *J. Geophys. Res. Ocean.* 122, 4569–4586. doi: 10.1002/2016JC012441

Moksness, E., and Pavlov, D. A. (1996). Management by life cycle of wolffish, *Anarhichas lupus L.*, a new species for cold-water aquaculture: a technical paper. *Aquacult. Res.* 27, 865–883.

Nahrgang, J., Varpe, Ø., Korshunova, E., Murzina, S., Hallanger, I. G., Vieweg, I., et al. (2014). Gender specific reproductive strategies of an Arctic key species (*Boreogadus saida*) and implications of climate change. *PLoS ONE.* 9:452. doi: 10.1371/journal.pone.0098452

Naito, Y., Costa, D. P., Adachi, T., Robinson, P. W., Fowler, M., and Takahashi, A. (2013). Unravelling the mysteries of a mesopelagic diet: a large apex predator specializes on small prey. *Funct. Ecol.* 27, 710–717. doi: 10.1111/1365-2435.12083

Nenadić, O., and Greenacre, M. (2007). Correspondence analysis in R, with two- and three-dimensional graphics: the ca package. *J. Stat. Soft.* 20:13. doi: 10.18637/jss.v020.i03

Pepin, P. (2013). Distribution and feeding of *Benthosema glaciale* in the western Labrador Sea: Fish–zooplankton interaction and the consequence to calanoid copepod populations. *Deep-Sea Res. Part I.* 75, 119–134. doi: 10.1016/j.dsr.2013.01.012

Petursdottir, H., Gislason, A., and Falk-Petersen, S. (2008). Lipid classes and fatty acid compositions of muscle, liver and skull oil in deep-sea redfish *Sebastes mentella* over the Reykjanes Ridge. *J. Fish Biol.* 73, 2485–2496. doi: 10.1111/j.1095-8649.2008.02100.x

Planque, B., Kristinsson, K., Astakhov, A., Bernreuther, M., Bethke, E., Drevetnyak, K., et al. (2013). Monitoring beaked redfish (*Sebastes mentella*) in the North Atlantic, current challenges and future prospects. *Aquat. Living Res.* 26, 293–306. doi: 10.1051/alr/2013062

Polyakov, I. V., Pnyushkov, A. V., Alkire, M. B., Ashik, I. M., Baumann, T. M., Carmack, E. C., et al. (2017). Greater role for Atlantic inflows on sea-ice loss in the Eurasian Basin of the Arctic Ocean. *Science.* 356, 285–291. doi: 10.1126/science.aai8204

Proud, R., Cox, M. J., Le Guen, C., and Brierley, A. S. (2018). Fine-scale depth structure of pelagic communities throughout the global ocean based on acoustic sound scattering layers. *Mar. Ecol. Prog. Ser.* 598, 35–48. doi: 10.3354/meps12612

Proud, R., Cox, M. J., Wotherspoon, S., and Brierley, A. S. (2015). A method for identifying sound scattering layers and extracting key characteristics. *Meth. Ecol. Evol.* 6, 1190–1198. doi: 10.1111/2041-210X.12396

Renaud, P. E., Berge, J., Varpe, Ø., Lønne, O. J., Nahrgang, J., Ottesen, C., et al. (2012). Is the poleward expansion by Atlantic cod and haddock threatening native polar cod, *Boreogadus saida*? *Polar Biol.* 35, 401–412. doi: 10.1007/s00300-011-1085-z

Rose, G. A. (1998). Acoustic target strength of capelin in Newfoundland waters. *ICES J. Mar. Sci.* 55, 918–923. doi: 10.1006/jmsc.1998.0358

Rose, G. A., and Porter, D. R. (1996). Target-strength studies on Atlantic cod (*Gadus morhua*) in Newfoundland waters. *ICES J. Mar. Sci.* 53, 259–265. doi: 10.1006/jmsc.1996.0032

Ryan, T. E., Downie, R. A., Kloser, R. J., and Keith, G. (2015). Reducing bias due to noise and attenuation in open-ocean echo integration data. *ICES J. Mar. Sci.* 72, 2482–2493. doi: 10.1093/icesjms/fsv121

Sargent, J. R., and Falk-Petersen, S. (1981). Ecological investigations on the zooplankton community in Balsfjorden, Northern Norway - Lipids and fatty acids in *Meganyctiphanes norvegica*, T*hysanoessa raschi* and *Thysanoessa inermis* during mid-winter. *Mar. Biol.* 62, 131–137.

Scoulding, B., Chu, D., Ona, E., and Fernandes, P. G. (2015). Target strengths of two abundant mesopelagic fish species. *J. Acoust. Soc. Am.* 137, 989–1000. doi: 10.1121/1.4906177

Siegelman-Charbit, L., and Planque, B. (2016). Abundant mesopelagic fauna at oceanic high latitudes. *Mar. Ecol. Prog. Ser.* 546, 277–282. doi: 10.3354/meps11661

Simmonds, E. J., and MacLennan, D. N. (2005). *Fisheries Acoustics*. Oxford: Blackwell Science.

Stanton, T. K., Wiebe, P. H., Chu, D., Benfield, M. C., Scanlon, L., Martin, L., et al. (1994). On acoustic estimates of zooplankton biomass. *ICES J. Mar. Sci.* 51, 505–512. doi: 10.1006/jmsc.1994.1051

St. John, M. A., Borja, A., Chust, G., Heath, M., Grigorov, I., Mariani, P., et al. (2016). A dark hole in our understanding of marine ecosystems and their services: perspectives from the mesopelagic community. *Front. Mar. Sci.* 3:0031. doi: 10.3389/fmars.2016.00031

van Leeuwe, M. A., Tedesco, L., Arrigo, K. R., Assmy, P., Campbell, K., Meiners, K. M., et al. (2018). Microalgal community structure and primary production in Arctic and Antarctic sea ice: a synthesis. *Elementa. Sci. Anthrop.* 6. p.4. doi: 10.1525/elementa.267

Wassmann, P., Kosobokova, K. N., Slagstad, D., Drinkwater, K. F., Hopcroft, R. R., Moore, S. E., et al. (2015). The contiguous domains of Arctic Ocean advection: Trails of life and death. *Prog. Oceanogr.* 139, 42–65. doi: 10.1016/j.pocean.2015.06.011

Yasuma, H., Sawada,K., Takao, Y., and Miyashita, K., Aoki, I. (2010). Swimbladder condition and target strength of myctophid fish in the temperate zone of the Northwest Pacific. *ICES J. Mar. Sci.* 67, 135–144. doi: 10.1093/icesjms/fsp218

Conflict of Interest Statement: The authors declare that the research was conducted in the absence of any commercial or financial relationships that could be construed as a potential conflict of interest.